Abstract

In bioengineering applications problems of flow interacting with elastic solid are very common. We formulate the problem of interaction for an incompressible fluid and an incompressible elastic material in a fully coupled arbitrary Lagrangian-Eulerian formulation. The mathematical description and the numerical schemes are designed in such a way that more complicated constitutive relations (and more realistic for bioengineering applications) can be incorporated easily. The whole domain of interest is treated as one continuum and the same discretization in space (Q2/P1 FEM) and time (Crank-Nicholson) is used for both, solid and fluid, parts. The resulting nonlinear algebraic system is solved by an approximate Newton method. The combination of second order discretization and fully coupled solution method gives a method with high accuracy and robustness. To demonstrate the flexibility of this numerical approach we apply the same method to a mixture based model of elastic material with perfusion which also falls into the category of fluid structure interactions. A few simple 2D example calculations with simple material models and a large deformations of the solid part are presented.

Fluid-structure interaction with applications in biomechanics

J. Hron
University of Dortmund, Institute of Applied Mathematics,
Vogelpothsweg 87, 44227 Dortmund, Germany

1 Overview

Both problems of viscous fluid flow and of elastic body deformation have been studied separately for many years in great detail. But there are many problems encountered in real life where an interaction between those two medias is of great importance. Typical example of such a problem is the area of aero-elasticity. Another important area where such interaction is of great interest is the biomechanics. Such interaction is encountered especially when dealing with the blood circulatory system. Problem of a pulsative flow in an elastic tube, flow through the heart flaps, flow in the heart chambers are some of the examples. In all these cases we have to deal with large deformations of a deformable solid interacting with an unsteady, often periodic, fluid flow. The ability to model and predict the mechanical behavior of biological tissues is very important in several areas of bio-engineering and medicine. For example, a good mathematical model for biological tissue could be used in such areas as early recognition or prediction of heart muscle failure, advanced design of new treatments and operative procedures, and the understanding of atherosclerosis and associated problems. Other possible applications include development of virtual reality programs for training new surgeons or designing new operative procedures (see Miga et al. [1998], Paulsen et al. [1999]), and last but not least the design of medical instruments or artificial replacements with optimal mechanical and other properties as close as possible to the original parts (see Zoppou et al. [1997]). These are some of the areas where a good mathematical model of soft tissue with reliable and fast numerical solution is essential for success.

1.1 Fluid structure models

There have been several different approaches to the problem of fluid-structure interaction. Most notably the work of Peskin and McQueen [1989], Peskin [1982], Peskin and McQueen [1980], Peskin [1977] where an immersed boundary method was developed and applied to a three-dimensional model of the heart. In this model they consider a set of one-dimensional elastic fibers immersed in three-dimensional fluid region and using parallel supercomputer they were able to model the pulse of the heart ventricle. Their method can capture the anisotropy caused by the muscle fibers.

A fluid-structure model with the wall modeled as a thin shell was used to model the left heart ventricle in Costa et al. [1996a,b] and Quarteroni et al. [2000], Quarteroni [2001]. In Heil [1997, 1998] similar approach was used to model a flow in a collapsible tubes. In these models the wall is modeled by two-dimensional thin shell which can be modified to capture the anisotropy of the muscle. In reality the thickness of the wall can be significant and very important. For example in arteries the wall thickness can be up to 30% of the diameter and its local thickening can be the cause of an aneurysm creation. In the case of heart ventricle the thickness of the wall is also significant and also the direction of the muscle fibers changes through the wall.

1.2 Mixture models for perfusion

Another class of models which fall into the fluid structure interaction problems are the fluid-solid mixture models used for simulation of soft tissue perfusion like muscles or cartelage. Mixture theory was first applied to swelling and diffusion in rubber materials Dai and Rajagopal [1990], Rajagopal and Tao [1995], mechanics of skin Oomens and van Campen [1987], compression of cartilage Spilker et al. [1988], Kwan et al. [1990], Reynolds and Humphrey [1998] and blood perfusion through biological tissues in Vankan et al. [1996, 1997]. (see for example Fung [1993] and Maurel et al. [1998]) The basic idea of mixture theory is the assumption of co-occupancy, i.e., at each spatial point there is certain fraction of each constituent (with associated fields) and there are prescribed balance equations for each constituent of the mixture as is usual for a single continuum, with additional terms representing the interaction between constituents within the mixture.

There have been several numerical studies of mixture models. One dimensional diffusion of fluid through an isotropic material is solved in Shi [1973], for transversely isotropic materials in Dai and Rajagopal [1990] and in Reynolds and Humphrey [1998] a one dimensional diffusion through isotropic stretched slab is solved using a velocity boundary condition. Finite element solutions of mixture models for the small deformation, linear elastic case are presented in Kwan et al. [1990], Vankan et al. [1997] and for nonlinear large deformation description of various soft tissues in Spilker et al. [1988], Spilker and Suh [1990], Suh et al. [1991], Donzelli et al. [1992], Vermilyea and Spilker [1993], Almeida and Spilker [1998], Levenston et al. [1998].

1.3 Theoretical results

The theoretical investigation of the fluid structure interaction problems is complicated by the need of mixed description. While for the solid part the natural view is the material (Lagrangian) description for the fluid it is the spatial

(Eulerian) description. In the case of their combination some kind of mixed description (usually refered to as the arbitrary Lagrangian-Eulerian description) has to be used which brings additional nonlinearity into the resulting equations.

In Le Tallec and Mani [2000] a time dependent, linearized model of interaction between a viscous fluid and an elastic shell in small displacement approximation and its discretization is analyzed. The problem is further simplified by neglecting all changes in the geometry configuration. Under these simplifications by using the energy estimates they are able to show that the proposed formulation is well posed and a global weak solution exists. Further they show that an independent discretization by standard mixed finite elements for the fluid and by nonconforming DKT finite elements for the shell together with backward or central difference approximation of the time derivatives converges to the solution of the continuous problem.

In Rumpf [1998] a steady problem of equilibrium of an elastic fixed obstacle surrounded by a viscous fluid is studied. Existence of an equilibrium state is show with the displacement and velocity in $C^{2,\alpha}$ and pressure in $C^{1,\alpha}$ under assumption of small data in $C^{2,\alpha}$ and the domain boundaries of class C^3.

For basic introduction and complete reference of continuum theory see Gurtin [1981], Truesdell [1991], Maršík [1999], Haupt [2000]. Its application in biomechanics are presented in Fung [1993] and Maršík and Dvořák [1998] for example. We will mention in the following sections the basic notation and setup used in this work.

A numerical solution of the resulting equations of the fluid structure interaction problem poses great challenge since it includes the features of nonlinear elasticity, fluid mechanics and their coupling. The easiest solution strategy, mostly used in the available software packages, is to decouple the problem into the fluid part and solid part, for each of those parts to use some well established method of solution then the interaction is introduced as external boundary conditions in each of the subproblems. This has an advantage that there are many well tested finite element based numerical methods for separate problems of fluid flow and elastic deformation, on the other hand the treatment of the interface and the interaction is problematic. The approach presented here treats the problem as a single continuum with the coupling automatically taken care of as internal interface, which in our formulation does not require any special treatment.

2 Continuum description

Let $\Omega \subset \mathbb{R}^3$ be a reference configuration of a given body, possibly an abstract one. Let $\Omega_t \subset \mathbb{R}^3$ be a configuration of this body at time t. Then one-to-one, sufficiently smooth mapping χ_Ω of the reference configuration Ω to the current configuration

$$\chi_\Omega : \Omega \times [0,T] \mapsto \Omega_t, \tag{1}$$

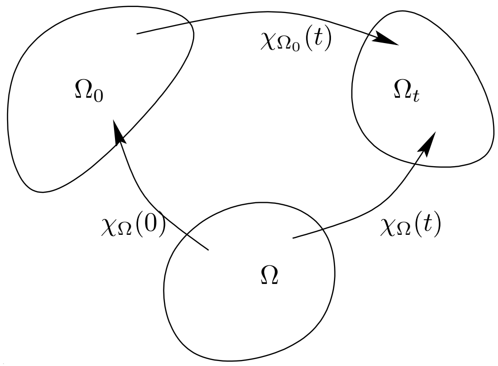

Figure 1: The referential domain Ω, initial Ω_0 and current state Ω_t and relations between them. The identification $\Omega \equiv \Omega_0$ is adopted in this text.

describes the motion of the body, see figure 1. The mapping χ_Ω depends on the choice of the reference configuration Ω which can be fixed in a various ways. Here we think of Ω to be the initial (stress-free) configuration Ω_0. Thus, if not emphasized, we mean by χ exactly $\chi_\Omega = \chi_{\Omega_0}$.

If we denote by $\mathbf{X}$ a material point in the reference configuration Ω then the position of this point at time t is given by

$$\mathbf{x} = \chi(\mathbf{X}, t). \tag{2}$$

Next, the mechanical fields describing the deformation are defined in a standard manner. The displacement field, the velocity field, deformation gradient and its determinant as

$$\mathbf{u}(\mathbf{X}, t) = \chi(\mathbf{X}, t) - \mathbf{X}, \qquad \mathbf{v} = \frac{\partial \chi}{\partial t}, \qquad \boldsymbol{F} = \frac{\partial \chi}{\partial \mathbf{X}}, \qquad J = \det \boldsymbol{F}. \tag{3}$$

Let us adopt following useful notations for some derivatives. Any field quantity φ with values in some vector space Y (i.e. scalar, vector or tensor valued) can be expressed in the Eulerian description as a function of the spatial position $\mathbf{x} \in \mathbb{R}^3$

$$\varphi = \tilde{\varphi}(\mathbf{x}, t) : \Omega_t \times [0, T] \mapsto Y.$$

Then we define following notations for the derivatives of the field φ

$$\frac{\partial \varphi}{\partial t} := \frac{\partial \tilde{\varphi}}{\partial t}, \qquad \nabla \varphi = \frac{\partial \varphi}{\partial \mathbf{x}} := \frac{\partial \tilde{\varphi}}{\partial \mathbf{x}}, \qquad \operatorname{div} \varphi := \operatorname{tr} \nabla \varphi. \tag{4}$$

In the case of Lagrangian description we consider the quantity φ to be defined on the reference configuration Ω, then for any $\mathbf{X} \in \Omega$ we can express the quantity φ as

$$\varphi = \bar{\varphi}(\mathbf{X}, t) : \Omega \times [0, T] \mapsto Y,$$

and we define the derivatives of the field φ as

$$\frac{d\varphi}{dt} := \frac{\partial \bar{\varphi}}{\partial t}, \qquad \operatorname{Grad} \varphi = \frac{\partial \varphi}{\partial \mathbf{X}} := \frac{\partial \bar{\varphi}}{\partial \mathbf{X}}, \qquad \operatorname{Div} \varphi := \operatorname{tr} \operatorname{Grad} \varphi. \tag{5}$$

These two descriptions can be related to each other through following relations

$$\bar{\varphi}(\mathbf{X}, t) = \tilde{\varphi}(\chi(\mathbf{X}, t), t), \tag{6}$$

$$\frac{d\varphi}{dt} = \frac{\partial \varphi}{\partial t} + (\nabla \varphi)\mathbf{v}, \qquad \operatorname{Grad} \varphi = (\nabla \varphi)\boldsymbol{F}, \qquad \int_{\Omega_t} \varphi dv = \int_{\Omega} \varphi J dV \tag{7}$$

$$\frac{d\boldsymbol{F}}{dt} = \operatorname{Grad} \mathbf{v}, \qquad \frac{\partial J}{\partial \boldsymbol{F}} = J\boldsymbol{F}^{-T}, \qquad \frac{dJ}{dt} = J \operatorname{div} \mathbf{v}. \tag{8}$$

For the formulation of the balance laws we will need to express a time derivatives of some integrals. The following series of equalities obtained by using the previously stated relations will be useful

$$\begin{aligned}
\frac{d}{dt}\int_{\Omega_t} \varphi dv =& \frac{d}{dt}\int_{\Omega} \varphi J dV = \int_{\Omega} \frac{d}{dt}(\varphi J)\, dV = \int_{\Omega_t} \left(\frac{d\varphi}{dt} + \varphi \operatorname{div} \mathbf{v}\right) dv \\
=& \int_{\Omega_t} \left(\frac{\partial \varphi}{\partial t} + \operatorname{div}(\varphi \mathbf{v})\right) dv = \int_{\Omega_t} \frac{\partial \varphi}{\partial t} dv + \int_{\partial \Omega_t} \varphi \mathbf{v} \cdot \mathbf{n} da \\
=& \frac{\partial}{\partial t}\int_{\Omega_t} \varphi dv + \int_{\partial \Omega_t} \varphi \mathbf{v} \cdot \mathbf{n} da.
\end{aligned} \tag{9}$$

And also the Piola identity will be used $\operatorname{Div}(J\boldsymbol{F}^{-T}) = \mathbf{0}$, which can be checked by differentiating the left hand side and using (8) together with an identity obtained by differentiating the relation $\boldsymbol{F}\boldsymbol{F}^{-1} = \boldsymbol{I}$.

2.1 Balance laws

In this section we will formulate the balance relations for mass and momentum in three forms: the Eulerian, the Lagrangian and the arbitrary Eulerian-Lagrangian (ALE) description.

The Eulerian (or spatial) description is well suited for a problem of fluid flowing through some spatially fixed region. In such a case the material particles can enter and leave the region of interest. The fundamental quantity describing the motion is the velocity vector.

On the other hand the Lagrangian (or referential) description is well suited for a problem of deforming a given body consisting of a fixed set of material particles. In this case the actual boundary of the body can change its shape. The fundamental quantity describing the motion in this case is the vector of displacement from the referential state.

In the case of fluid-structure interaction problem we can still use the Lagrangian description for the deformation of the solid part. The fluid flow now takes place in a domain with boundary given by the deformation of the structure which can change in time and is influenced back by the fluid flow. The mixed ALE description of the fluid has to be used in this case. The fundamental quantity describing the motion of the fluid is still the velocity vector but the description is accompanied by a certain displacement field which describes the change of the fluid domain. This displacement field has no connection to the fluid velocity field and the purpose of its introduction is to provide a transformation of the current fluid domain and corresponding governing equations to some fixed reference domain. This method is sometimes called a pseudo-solid mapping method [see Sackinger et al., 1996].

Let $\mathcal{P} \subset \mathbb{R}^3$ be a fixed region in space (control volume) with the boundary $\partial\mathcal{P}$ and unit outward normal vector $\mathbf{n}_{\mathcal{P}}$, such that

$$\mathcal{P} \subset \Omega_t \quad \text{for all } t \in [0, T].$$

Let ϱ denotes the mass density of the material. Then the balance of mass in the region $\mathcal{P}$ can be written as

$$\frac{\partial}{\partial t}\int_{\mathcal{P}} \varrho dv + \int_{\partial\mathcal{P}} \varrho \mathbf{v} \cdot \mathbf{n}_{\mathcal{P}} da = 0. \tag{10}$$

If all the fields are sufficiently smooth this equation can be written in local form with respect to the current configuration as

$$\frac{\partial \varrho}{\partial t} + \operatorname{div}(\varrho \mathbf{v}) = 0. \tag{11}$$

It will be useful to derive the mass balance equation from the Lagrangian point of view. Let $\mathcal{Q} \subset \Omega$ be a fixed set of particles. Then $\chi(\mathcal{Q}, t) \subset \Omega_t$ is a region occupied by these particles at the time t, and the balance of mass can be expressed as

$$\frac{d}{dt}\int_{\chi(\mathcal{Q},t)} \varrho dv = 0, \tag{12}$$

which in local form with respect to the reference configuration can be written as

$$\frac{d}{dt}(\varrho J) = 0. \tag{13}$$

In the case of arbitrary Lagrangian-Eulerian description we take a region $\mathcal{Z} \subset \mathbb{R}^3$ which is itself moving independently of the motion of the body. Let the motion of the control region $\mathcal{Z}$ be described by a given mapping

$$\zeta_{\mathcal{Z}} : \mathcal{Z} \times [0, T] \mapsto \mathcal{Z}_t, \qquad \mathcal{Z}_t \subset \Omega_t \quad \forall t \in [0, T],$$

with the corresponding velocity $\mathbf{v}_{\mathcal{Z}} = \frac{\partial \zeta_{\mathcal{Z}}}{\partial t}$, deformation gradient $\boldsymbol{F}_{\mathcal{Z}} = \frac{\partial \zeta_{\mathcal{Z}}}{\partial \mathbf{X}}$ and its determinant $J_{\mathcal{Z}} = \det \boldsymbol{F}_{\mathcal{Z}}$. The mass balance equation can be written as

$$\frac{\partial}{\partial t}\int_{\mathcal{Z}_t} \varrho dv + \int_{\partial\mathcal{Z}_t} \varrho(\mathbf{v} - \mathbf{v}_{\mathcal{Z}}) \cdot \mathbf{n}_{\mathcal{Z}_t} da = 0, \tag{14}$$

this can be viewed as Eulerian description with moving spatial coordinate system or as a grid deformation in the context of the finite element method. In order to obtain a local form of the balance relation we need to transform the integration to the fixed spatial region $\mathcal{Z}$

$$\frac{\partial}{\partial t}\int_{\mathcal{Z}} \varrho J_{\mathcal{Z}} dv + \int_{\partial \mathcal{Z}} \varrho(\mathbf{v} - \mathbf{v}_{\mathcal{Z}}) \cdot \boldsymbol{F}_{\mathcal{Z}}^{-T} \mathbf{n}_{\mathcal{Z}} J_{\mathcal{Z}} da = 0, \tag{15}$$

then the local form is

$$\frac{\partial}{\partial t}(\varrho J_{\mathcal{Z}}) + \operatorname{div}\left(\varrho J_{\mathcal{Z}}(\mathbf{v} - \mathbf{v}_{\mathcal{Z}}) \boldsymbol{F}_{\mathcal{Z}}^{-T}\right) = 0. \tag{16}$$

The two previous special formulations can be now recovered. If the region $\mathcal{Z}$ is not moving in space, i.e. $\mathcal{Z} = \mathcal{Z}_t, \forall t \in [0, T]$, then $\zeta_{\mathcal{Z}}$ is the identity mapping, $\boldsymbol{F}_{\mathcal{Z}} = \boldsymbol{I}, J_{\mathcal{Z}} = 1, \mathbf{v}_{\mathcal{Z}} = \mathbf{0}$ and (16) reduces to (11). While, if the region $\mathcal{Z}$ moves exactly with the material, i.e. $\zeta_{\mathcal{Z}} = \chi|_{\mathcal{Z}}$ then $\boldsymbol{F}_{\mathcal{Z}} = \boldsymbol{F}, J_{\mathcal{Z}} = J, \mathbf{v}_{\mathcal{Z}} = \mathbf{v}$ and (16) reduces to (13).

The balance of linear momentum is postulated in a similar way. Let $\boldsymbol{\sigma}$ denote the Cauchy stress tensor field, representing the surface forces per unit area, $\mathbf{f}$ be the body forces acting on the material per its unit mass. Then the balance of linear momentum in the Eulerian description is stated as

$$\frac{\partial}{\partial t}\int_{\mathcal{P}} \varrho \mathbf{v} dv + \int_{\partial \mathcal{P}} \varrho \mathbf{v} \otimes \mathbf{v} \mathbf{n}_{\mathcal{P}} da = \int_{\partial \mathcal{P}} \boldsymbol{\sigma}^T \mathbf{n}_{\mathcal{P}} da + \int_{\mathcal{P}} \varrho \mathbf{f} dv. \tag{17}$$

The local form of the linear momentum balance is

$$\frac{\partial \varrho \mathbf{v}}{\partial t} + \operatorname{div}(\varrho \mathbf{v} \otimes \mathbf{v}) = \operatorname{div} \boldsymbol{\sigma}^T + \varrho \mathbf{f}, \tag{18}$$

or with the use of (11) we can write

$$\varrho \frac{\partial \mathbf{v}}{\partial t} + \varrho(\nabla \mathbf{v})\mathbf{v} = \operatorname{div} \boldsymbol{\sigma}^T + \varrho \mathbf{f}. \tag{19}$$

From the Lagrangian point of view the momentum balance relation is

$$\frac{d}{dt}\int_{\chi(Q,t)} \varrho \mathbf{v} dv = \int_{\partial \chi(Q,t)} \boldsymbol{\sigma}^T \mathbf{n}_{\chi(Q,t)} da + \int_{\chi(Q,t)} \varrho \mathbf{f} dv. \tag{20}$$

Let us denote by $\boldsymbol{P} = J \boldsymbol{\sigma}^T \boldsymbol{F}^{-T}$ the first Piola-Kirchhoff stress tensor [see Gurtin, 1981], then the local form of the momentum balance is

$$\frac{d}{dt}(\varrho J \mathbf{v}) = \operatorname{Div} \boldsymbol{P} + \varrho J \mathbf{f}, \tag{21}$$

or using (13) we can write

$$\varrho J \frac{d\mathbf{v}}{dt} = \operatorname{Div} \boldsymbol{P} + \varrho J \mathbf{f}. \tag{22}$$

In the arbitrary Lagrangian-Eulerian formulation we obtain

$$\frac{\partial}{\partial t}\int_{\mathcal{Z}_t} \varrho \mathbf{v} dv + \int_{\partial \mathcal{Z}_t} \varrho \mathbf{v} \otimes (\mathbf{v} - \mathbf{v}_{\mathcal{Z}})\mathbf{n}_{\mathcal{Z}_t} da = \int_{\partial \mathcal{Z}_t} \boldsymbol{\sigma}^T \mathbf{n}_{\mathcal{Z}_t} da + \int_{\mathcal{Z}_t} \varrho \mathbf{f} dv, \quad (23)$$

which in the local form gives

$$\frac{\partial \varrho J_{\mathcal{Z}} \mathbf{v}}{\partial t} + \operatorname{div}\left(\varrho J_{\mathcal{Z}} \mathbf{v} \otimes (\mathbf{v} - \mathbf{v}_{\mathcal{Z}}) \boldsymbol{F}_{\mathcal{Z}}^{-T}\right) = \operatorname{div}\left(J_{\mathcal{Z}} \boldsymbol{\sigma}^T \boldsymbol{F}_{\mathcal{Z}}^{-T}\right) + \varrho J_{\mathcal{Z}} \mathbf{f}, \quad (24)$$

or with the use of (16) we can write

$$\varrho J_{\mathcal{Z}} \frac{\partial \mathbf{v}}{\partial t} + \varrho J_{\mathcal{Z}} (\nabla \mathbf{v}) \boldsymbol{F}_{\mathcal{Z}}^{-T} (\mathbf{v} - \mathbf{v}_{\mathcal{Z}}) = \operatorname{div}\left(J_{\mathcal{Z}} \boldsymbol{\sigma}^T \boldsymbol{F}_{\mathcal{Z}}^{-T}\right) + \varrho J_{\mathcal{Z}} \mathbf{f}. \quad (25)$$

In the case of angular momentum balance we assume that there are no external or internal sources of angular momentum, then it follows that the Cauchy stress tensor has to be symmetric, i.e. $\boldsymbol{\sigma} = \boldsymbol{\sigma}^T$. Assuming an isothermal conditions the energy balance is satisfied and the choice of the constitutive relations for the materials has to be compatible with the balance of entropy. [see Truesdell, 1991]

3 Fluid structure interaction problem formulation

At this point we make a few assumptions that will allow us to deal with the task of setting up a tractable problem. We will use the superscripts ^{s} and ^{f} to denote the quantities connected with the solid and fluid. Let us assume that the both materials are incompressible and all the processes are isothermal, which is well accepted approximation in biomechanics and let us denote the constant densities of each material by ϱ^f, ϱ^s.

3.1 Monolithic description

We denote by Ω_t^f the domain occupied by the fluid and Ω_t^s by the solid at time $t \in [0, T]$. Let $\Gamma_t^0 = \bar{\Omega}_t^f \cap \bar{\Omega}_t^s$ be the part of the boundary where the solid interacts with the fluid and $\Gamma_t^i, i = 1, 2, 3$ be the remaining external boundaries of the solid and the fluid as depicted in figure 2.

Let the deformation of the solid part be described by the mapping χ^s

$$\chi^s : \Omega^s \times [0, T] \mapsto \Omega_t^s, \quad (26)$$

with the corresponding displacement $\mathbf{u}^s$ and the velocity $\mathbf{v}^s$ given by

$$\mathbf{u}^s(\mathbf{X}, t) = \chi^s(\mathbf{X}, t) - \mathbf{X}, \qquad \mathbf{v}^s(\mathbf{X}, t) = \frac{\partial \chi^s}{\partial t}(\mathbf{X}, t). \quad (27)$$

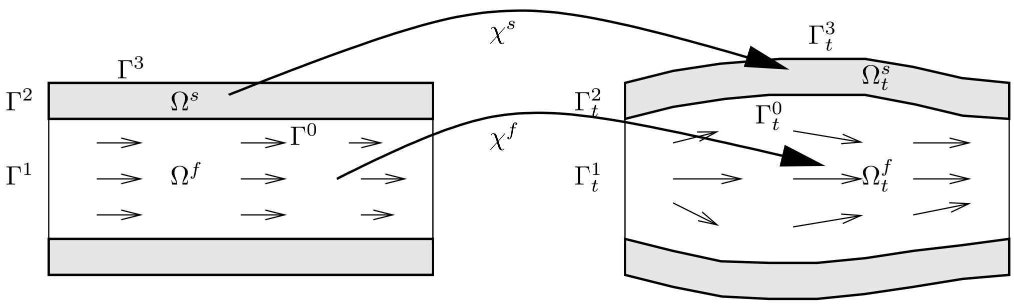

Figure 2: Undeformed (original) and deformed (current) configurations.

The fluid flow is described by the velocity field $\mathbf{v}^f$ defined on the fluid domain Ω_t^f

$$\mathbf{v}^f(\mathbf{x}, t) : \Omega_t^f \times [0, T] \mapsto \mathbb{R}^3. \tag{28}$$

Further we define the auxiliary mapping, denoted by ζ^f, to describe the change of the fluid domain and corresponding displacement $\mathbf{u}^f$ by

$$\zeta^f : \Omega^f \times [0, T] \mapsto \Omega_t^f, \qquad \mathbf{u}^f(\mathbf{X}, t) = \zeta^f(\mathbf{X}, t) - \mathbf{X}. \tag{29}$$

We require that the mapping ζ^f is sufficiently smooth, one to one and has to satisfy

$$\zeta^f(\mathbf{X}, t) = \chi^s(\mathbf{X}, t), \quad \forall(\mathbf{X}, t) \in \Gamma^0 \times [0, T]. \tag{30}$$

In the context of the finite element method this will describe the artificial mesh deformation inside the fluid region and it will be constructed as a solution to a suitable boundary value problem with (30) as the boundary condition.

The momentum and mass balance of the fluid in the time dependent fluid domain according to (16) and (24) are

$$\varrho^f \frac{\partial \mathbf{v}^f}{\partial t} + \varrho^f (\nabla \mathbf{v}^f)(\mathbf{v}^f - \frac{\partial \mathbf{u}^f}{\partial t}) = \operatorname{div} \boldsymbol{\sigma}^f \qquad \text{in } \Omega_t^f, \tag{31}$$

$$\operatorname{div} \mathbf{v}^f = 0 \qquad \text{in } \Omega_t^f, \tag{32}$$

together with the momentum (18) and mass (11) balance of the solid in the solid domain

$$\varrho^s \frac{\partial \mathbf{v}^s}{\partial t} + \varrho^s (\nabla \mathbf{v}^s)\mathbf{v}^s = \operatorname{div} \boldsymbol{\sigma}^s \qquad \text{in } \Omega_t^s, \tag{33}$$

$$\operatorname{div} \mathbf{v}^s = 0 \qquad \text{in } \Omega_t^s. \tag{34}$$

The interaction is due to the exchange of momentum through the common part of the boundary Γ_t^0. On this part we require that the forces are in balance and simultaneously the no slip boundary condition for the fluid, i.e.

$$\boldsymbol{\sigma}^f \mathbf{n} = \boldsymbol{\sigma}^s \mathbf{n} \quad \text{on } \Gamma_t^0, \qquad \mathbf{v}^f = \mathbf{v}^s \quad \text{on } \Gamma_t^0. \tag{35}$$

The remaining external boundary conditions can be of the following kind. A natural boundary condition on the fluid inflow and outflow part Γ_t^1

$$\boldsymbol{\sigma}^f \mathbf{n} = p_B \mathbf{n} \text{ on } \Gamma_t^1, \tag{36}$$

with p_B given value. Alternatively we can prescribe a Dirichlet type boundary condition on the inflow or outflow part Γ_t^1

$$\mathbf{v}^f = \mathbf{v}_B \text{ on } \Gamma_t^1, \tag{37}$$

where $\mathbf{v}_B$ is given. The Dirichlet boundary condition is prescribed for the solid displacement at the part Γ_t^2

$$\mathbf{u}^s = \mathbf{0} \text{ on } \Gamma_t^2, \tag{38}$$

and the stress free boundary condition for the solid is applied at the part Γ_t^3

$$\boldsymbol{\sigma}^s \mathbf{n} = \mathbf{0} \text{ on } \Gamma_t^3. \tag{39}$$

We introduce the domain $\Omega = \Omega^f \cup \Omega^s$, where Ω^f, Ω^s are the domains occupied by the fluid and solid in the initial undeformed state, and two fields defined on this domain as

$$\mathbf{u} : \Omega \times [0,T] \to \mathbb{R}^3, \qquad \mathbf{v} : \Omega \times [0,T] \to \mathbb{R}^3,$$

such that the field $\mathbf{v}$ represents the velocity at the given point and $\mathbf{u}$ the displacement on the solid part and the artificial displacement in the fluid part, taking care of the fact that the fluid domain is changing with time,

$$\mathbf{v} = \begin{cases} \mathbf{v}^s & \text{on } \Omega^s, \\ \mathbf{v}^f & \text{on } \Omega^f, \end{cases} \qquad \mathbf{u} = \begin{cases} \mathbf{u}^s & \text{on } \Omega^s, \\ \mathbf{u}^f & \text{on } \Omega^f. \end{cases} \tag{40}$$

Due to the conditions (30) and (35) both fields are continuous across the interface Γ_t^0 and we can define global quantities on Ω as the deformation gradient and its determinant

$$\boldsymbol{F} = \boldsymbol{I} + \operatorname{Grad} \mathbf{u}, \qquad J = \det \boldsymbol{F}. \tag{41}$$

Using this notation the solid balance laws (33) and (34) can be expressed in the Lagrangian formulation with the initial configuration Ω^s as reference, cf. (21),

$$J \varrho^s \frac{d\mathbf{v}}{dt} = \operatorname{Div} \boldsymbol{P}^s \qquad \text{in } \Omega^s, \tag{42}$$

$$J = 1 \qquad \text{in } \Omega^s. \tag{43}$$

The fluid equations (31) and (32) are already expressed in the arbitrary Lagrangian-Eulerian formulation with respect to the time dependent region Ω_t^f, now we transform the equations to the fixed initial region Ω^f by the mapping ζ^f defined by (29)

$$\varrho^f \frac{\partial \mathbf{v}}{\partial t} + \varrho^f (\operatorname{Grad} \mathbf{v}) \boldsymbol{F}^{-1} (\mathbf{v} - \frac{\partial \mathbf{u}}{\partial t}) = J^{-1} \operatorname{Div}(J \boldsymbol{\sigma}^f F^{-T}) \qquad \text{in } \Omega^f, \tag{44}$$

$$\operatorname{Div}(J \mathbf{v} \boldsymbol{F}^{-T}) = 0 \qquad \text{in } \Omega^f. \tag{45}$$

It remains to prescribe some relation for the mapping ζ^f. In terms of the corresponding displacement $\mathbf{u}^f$ we formulate some simple relation together with the Dirichlet boundary conditions required by (30), for example

$$\frac{\partial \mathbf{u}}{\partial t} = \Delta \mathbf{u} \quad \text{in } \Omega^f, \qquad \mathbf{u} = \mathbf{u}^s \quad \text{on } \Gamma^0, \qquad \mathbf{u} = \mathbf{0} \quad \text{on } \Gamma^1. \tag{46}$$

Other choices are possible for example the mapping $\mathbf{u}^f$ can be realized as a solution of the elasticity problem with the same Dirichlet boundary conditions. [see Sackinger et al., 1996]

The complete set of the equations can be written as

$$\frac{\partial \mathbf{u}}{\partial t} = \begin{cases} \mathbf{v} & \text{in } \Omega^s, \\ \Delta \mathbf{u} & \text{in } \Omega^f, \end{cases} \tag{47}$$

$$\frac{\partial \mathbf{v}}{\partial t} = \begin{cases} \frac{1}{J\varrho^s} \operatorname{Div} \boldsymbol{P}^s & \text{in } \Omega^s, \\ -(\operatorname{Grad} \mathbf{v}) \boldsymbol{F}^{-1} (\mathbf{v} - \frac{\partial \mathbf{u}}{\partial t}) + \frac{1}{J\varrho^f} \operatorname{Div}(J \boldsymbol{\sigma}^f \boldsymbol{F}^{-T}) & \text{in } \Omega^f, \end{cases} \tag{48}$$

$$0 = \begin{cases} J - 1 & \text{in } \Omega^s, \\ \operatorname{Div}(J \mathbf{v} \boldsymbol{F}^{-T}) & \text{in } \Omega^f, \end{cases} \tag{49}$$

with the initial conditions

$$\mathbf{u}(0) = \mathbf{0} \quad \text{in } \Omega, \qquad \mathbf{v}(0) = \mathbf{v}_0 \quad \text{in } \Omega, \tag{50}$$

and boundary conditions

$$\mathbf{u} = \mathbf{0}, \quad \mathbf{v} = \mathbf{v}_B \quad \text{on } \Gamma^1, \qquad \mathbf{u} = \mathbf{0} \quad \text{on } \Gamma^2, \qquad \boldsymbol{\sigma}^s \mathbf{n} = \mathbf{0} \quad \text{on } \Gamma^3. \tag{51}$$

3.2 Constitutive equations

In order solve the balance equations we need to specify the constitutive relations for the stress tensors. For the fluid we use the incompressible Newtonian relation

$$\boldsymbol{\sigma}^f = -p^f \boldsymbol{I} + \mu (\nabla \mathbf{v}^f + (\nabla \mathbf{v}^f)^T), \tag{52}$$

where μ represents the viscosity of the fluid and p^f is the Lagrange multiplier corresponding to the incompressibility constraint (32).

For the solid part we assume that it can be described by an incompressible hyper-elastic material. We specify the Helmholtz potential Ψ and the solid stress is given by

$$\boldsymbol{\sigma}^s = -p^s \boldsymbol{I} + \varrho^s \frac{\partial \Psi}{\partial \boldsymbol{F}} \boldsymbol{F}^T, \tag{53}$$

the first Piola-Kirchhoff stress tensor is then given by

$$\boldsymbol{P}^s = -Jp^s\boldsymbol{F}^{-T} + J\varrho^s\frac{\partial \Psi}{\partial \boldsymbol{F}}, \tag{54}$$

where p^s is the Lagrange multiplier corresponding to the incompressibility constraint (43).

The Helmholtz potential can be expressed as a function of different quantities

$$\Psi = \hat{\Psi}(\boldsymbol{F}) = \hat{\Psi}(\boldsymbol{I} + \mathrm{Grad}\,\mathbf{u}),$$

but due to the principle of material frame indifference the Helmholtz potential Ψ depends on the deformation only through the right Cauchy-Green deformation tensor $\boldsymbol{C} = \boldsymbol{F}^T\boldsymbol{F}$ [see Gurtin, 1981]

$$\Psi = \tilde{\Psi}(\boldsymbol{C}). \tag{55}$$

A certain coerciveness condition is usually imposed on the form of the Helmholtz potential

$$\bar{\Psi}(\mathrm{Grad}\,\mathbf{u}(\mathbf{X},t)) \geq a\,\|\mathrm{Grad}\,\mathbf{u}(\mathbf{X},t)\|^2 - b(\mathbf{X}), \tag{56}$$

where a is a positive constant and $b \in L^1(\Omega^s)$. With this assumption and using the integral identity (65) we can derive an energy estimate of the following form

$$\begin{aligned}\frac{c}{2}\|\mathbf{v}(T)\|^2_{L^2(\Omega_T)} + \int_0^T \mu\,\|\nabla\mathbf{v}\|^2_{L^2(\Omega_t^f)}\,dt + a\,\|\mathrm{Grad}\,\mathbf{u}(T)\|^2_{L^2(\Omega^s)} \\ \leq \|b\|_{L^1(\Omega^s)} + \frac{1}{2}\|\mathbf{v}_0\|^2_{L^2(\Omega^f)} + \frac{\beta}{2}\|\mathbf{v}_0\|^2_{L^2(\Omega^s)}.\end{aligned} \tag{57}$$

where $c = \min(1,\beta)$.

Typical examples for the Helmholtz potential used for isotropic materials like rubber is the Mooney-Rivlin material

$$\tilde{\Psi} = c_1(I_C - 3) + c_2(II_C - 3), \tag{58}$$

where $I_C = \mathrm{tr}\,\boldsymbol{C}, II_C = \mathrm{tr}\,\boldsymbol{C}^2 - \mathrm{tr}^2\,\boldsymbol{C}, III_C = \det\boldsymbol{C}$ are the invariants of the right Cauchy-Green deformation tensor $\boldsymbol{C}$ and c_i are some material constants. A special case of neo-Hookean material is obtained for $c_2 = 0$. With a suitable choice of the material parameters the entropy inequality and the balance of energy is automatically satisfied.

3.3 Weak formulation

We non-dimensionalize all the quantities by a given characteristic length L and speed V as follows

$$\hat{t} = t\frac{V}{L}, \qquad \hat{\mathbf{x}} = \frac{\mathbf{x}}{L}, \qquad \hat{\mathbf{u}} = \frac{\mathbf{u}}{L}, \qquad \hat{\mathbf{v}} = \frac{\mathbf{v}}{V},$$

$$\hat{\boldsymbol{\sigma}}^s = \boldsymbol{\sigma}^s\frac{L}{\varrho^f V^2}, \qquad \hat{\boldsymbol{\sigma}}^f = \boldsymbol{\sigma}^f\frac{L}{\varrho^f V^2}, \qquad \hat{\mu} = \frac{\mu}{\varrho^f V L}, \qquad \hat{\Psi} = \Psi\frac{L}{\varrho^f V^2},$$

further using the same symbols, without the hat, for the non-dimensional quantities and denoting by $\beta = \frac{\varrho^s}{\varrho^f}$ the densities ratio. The non-dimensionalized system with the choice of material relations, (52) for viscous fluid and (54) for the hyper-elastic solid is

$$\frac{\partial \mathbf{u}}{\partial t} = \begin{cases} \mathbf{v} & \text{in } \Omega^s, \\ \Delta \mathbf{u} & \text{in } \Omega^f, \end{cases} \tag{59}$$

$$\frac{\partial \mathbf{v}}{\partial t} = \begin{cases} \frac{1}{\beta} \operatorname{Div}\left(-Jp^s \boldsymbol{F}^{-T} + \frac{\partial \Psi}{\partial \boldsymbol{F}}\right) & \text{in } \Omega^s, \\ -(\operatorname{Grad} \mathbf{v})\boldsymbol{F}^{-1}(\mathbf{v} - \frac{\partial \mathbf{u}}{\partial t}) + \operatorname{Div}\left(-Jp^f \boldsymbol{F}^{-T} + J\mu \operatorname{Grad} \mathbf{v} \boldsymbol{F}^{-1} \boldsymbol{F}^{-T}\right) & \text{in } \Omega^f, \end{cases} \tag{60}$$

$$0 = \begin{cases} J - 1 & \text{in } \Omega^s, \\ \operatorname{Div}(J\mathbf{v}\boldsymbol{F}^{-T}) & \text{in } \Omega^f, \end{cases} \tag{61}$$

and the boundary conditions

$$\boldsymbol{\sigma}^f \mathbf{n} = \boldsymbol{\sigma}^s \mathbf{n} \quad \text{on } \Gamma_t^0, \qquad \mathbf{v} = \mathbf{v}_B \quad \text{on } \Gamma_t^1, \tag{62}$$

$$\mathbf{u} = \mathbf{0} \quad \text{on } \Gamma_t^2, \qquad \boldsymbol{\sigma}^f \mathbf{n} = \mathbf{0} \quad \text{on } \Gamma_t^3. \tag{63}$$

Let $I = [0, T]$ denote the time interval of interest. We multiply the equations (59)-(61) by the test functions ζ, ξ, γ such that $\zeta = \mathbf{0}$ on Γ^2, $\xi = \mathbf{0}$ on Γ^1 and integrate over the space domain Ω and the time interval I. Using integration by parts on some of the terms and the boundary conditions we obtain

$$\int_0^T \int_\Omega \frac{\partial \mathbf{u}}{\partial t} \cdot \zeta dV dt = \int_0^T \int_{\Omega^s} \mathbf{v} \cdot \zeta dV dt - \int_0^T \int_{\Omega^f} \operatorname{Grad} \mathbf{u} \cdot \operatorname{Grad} \zeta dV dt, \tag{64}$$

$$\begin{aligned} \int_0^T \int_{\Omega^f} J \frac{\partial \mathbf{v}}{\partial t} \cdot \xi dV dt &+ \int_0^T \int_{\Omega^s} \beta J \frac{\partial \mathbf{v}}{\partial t} \cdot \xi dV dt \\ &= - \int_0^T \int_{\Omega^f} J \operatorname{Grad} \mathbf{v} \boldsymbol{F}^{-1} (\mathbf{v} - \frac{\partial \mathbf{u}}{\partial t}) \cdot \xi dV dt \\ &\quad + \int_0^T \int_\Omega Jp \boldsymbol{F}^{-T} \cdot \operatorname{Grad} \xi dV dt \\ &\quad - \int_0^T \int_{\Omega^s} \frac{\partial \Psi}{\partial \boldsymbol{F}} \cdot \operatorname{Grad} \xi dV dt \\ &\quad - \int_0^T \int_{\Omega^f} J\mu \operatorname{Grad} \mathbf{v} \boldsymbol{F}^{-1} \boldsymbol{F}^{-T} \cdot \operatorname{Grad} \xi dV dt, \end{aligned} \tag{65}$$

$$0 = \int_0^T \int_{\Omega^s} (J - 1)\gamma dV dt + \int_0^T \int_{\Omega^f} \operatorname{Div}(J\mathbf{v}\boldsymbol{F}^{-T})\gamma dV dt. \tag{66}$$

Let us define the following spaces

$$
\begin{aligned}
U &= \{\mathbf{u} \in L^\infty(I, [W^{1,2}(\Omega)]^3), \mathbf{u} = \mathbf{0} \text{ on } \Gamma^2\}, \\
V &= \{\mathbf{v} \in L^2(I, [W^{1,2}(\Omega_t)]^3) \cap L^\infty(I, [L^2(\Omega_t)]^3), \mathbf{v} = \mathbf{0} \text{ on } \Gamma^1\}, \\
P &= \{p \in L^2(I, L^2(\Omega))\},
\end{aligned}
$$

then the variational formulation of the fluid-structure interaction problem is stated as follows

Definition 67 *Find* $(\mathbf{u}, \mathbf{v} - \mathbf{v}_B, p) \in U \times V \times P$ *such that equations* (64), (65) *and* (66) *are satisfied for all* $(\zeta, \xi, \gamma) \in U \times V \times P$.

3.4 Discretization

From now on, we restrict ourselves to two dimensions. This restriction is due to an easier presentation and the computational time needed to solve the problem. Apart of these two reasons, the same discretization procedure can be applied to the three dimensional problem.

The time discretization is done by the Crank-Nicholson scheme which is only conditionally stable but it has better conservation property than for example the implicit Euler scheme [see Farhat et al., 1995, Koobus and Farhat, 1999]. The Crank-Nicholson scheme can be obtained by dividing the time interval I into the series of time steps $[t^n, t^{n+1}]$ with step length $k_n = t^{n+1} - t^n$. Assuming that the test functions are piecewise constant on each time step $[t^n, t^{n+1}], \forall n$, writing the weak formulation (64)-(65) for the time interval $[t^n, t^{n+1}]$, approximating the time derivatives by the central differences

$$
\frac{\partial f}{\partial t} \approx \frac{f(t^{n+1}) - f(t^n)}{k_n} \tag{68}
$$

and approximating the time integration for the remaining terms by the trapezoidal quadrature rule as

$$
\int_{t^n}^{t^{n+1}} f(t)dt \approx \frac{k_n}{2}(f(t^n) + f(t^{n+1})), \tag{69}
$$

we obtain the time discretized system. The last equation was taken explicitly for the time t^{n+1} and the corresponding term with the Lagrange multiplier p_h^n in the equation (65) was also taken explicitly.

The discretization in space is done by the finite element method. We approximate the domain Ω by a domain Ω_h with polygonal boundary and by $\mathcal{T}_h$ we denote a set of quadrilaterals covering the domain Ω_h. We assume that $\mathcal{T}_h$ is regular in the sense that any two quadrilateral are disjoint or have a common vertex or a common edge. By $\bar{T} = [-1, 1]^2$ we denote the reference quadrilateral.

Our treatment of the problem as a one system suggests to use the same finite elements on both, the solid part and the fluid region. Since both materials are incompressible we have to choose a pair of finite element spaces know to be stable

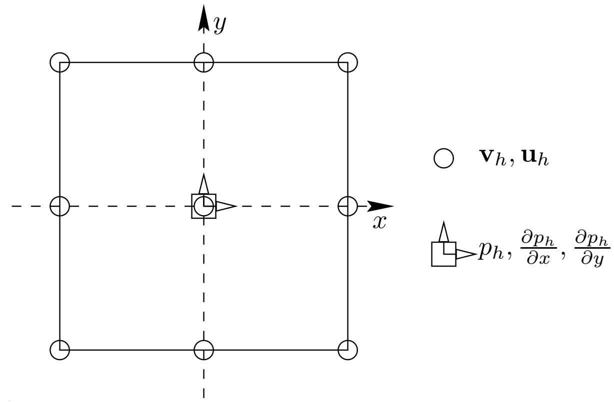

Figure 3: Location of the degrees of freedom for the Q_2, P_1 element

for the problems with incompressibility constraint. One possible choice is the conforming biquadratic, discontinuous bilinear Q_2, P_1 pair, see figure 3 for the location of the degrees of freedom. This choice results to 39 degrees of freedom on an element in the case of our displacement, velocity, pressure formulation in two dimensions and to 112 degrees of freedom on an element in three dimensions. This seems rather prohibitive, especially for a three dimensional computation.

The spaces U, V, P on an interval $[t^n, t^{n+1}]$ would be approximated in the case of Q_2, Q_1 pair as

$$
\begin{aligned}
U_h &= \{\mathbf{u}_h \in [C(\Omega_h)]^2, \mathbf{u}_h|_T \in [Q_2(T)]^2 \quad \forall T \in \mathcal{T}_h, \mathbf{u}_h = \mathbf{0} \text{ on } \Gamma_2\},\\
V_h &= \{\mathbf{v}_h \in [C(\Omega_h)]^2, \mathbf{v}_h|_T \in [Q_2(T)]^2 \quad \forall T \in \mathcal{T}_h, \mathbf{v}_h = 0 \text{ on } \Gamma_1\},\\
P_h &= \{p_h \in L^2(\Omega_h), p_h|_T \in P_1(T) \quad \forall T \in \mathcal{T}_h\}.
\end{aligned}
$$

Let us denote by $\mathbf{u}_h^n$ the approximation of $\mathbf{u}(t^n)$, $\mathbf{v}_h^n$ the approximation of $\mathbf{v}(t^n)$ and p_h^n the approximation of $p(t^n)$. Further we will use following shorthand notation

$$
\begin{gathered}
\boldsymbol{F}^n = \boldsymbol{I} + \operatorname{Grad}\mathbf{u}_h^n, \quad J^n = \det \boldsymbol{F}^n \quad J^{n+\frac{1}{2}} = \frac{1}{2}(J^n + J^{n+1}),\\
(f,g) = \int_\Omega f \cdot g dV, \quad (f,g)_s = \int_{\Omega^s} f \cdot g dV, \quad (f,g)_f = \int_{\Omega^f} f \cdot g dV,
\end{gathered}
$$

f, g being scalars, vectors or tensors.

Writing down the discrete equivalent of the equations (64)-(66) yields

$$
\begin{aligned}
\left(\mathbf{u}_h^{n+1}, \eta\right) - \frac{k_n}{2}\Big\{ \left(\mathbf{v}_h^{n+1}, \eta\right)_s + \left(\nabla \mathbf{u}_h^{n+1}, \nabla \eta\right)_f \Big\}&\\
- \left(\mathbf{u}_h^n, \eta\right) - \frac{k_n}{2}\Big\{ \left(\mathbf{v}_h^n, \eta\right)_s + \left(\nabla \mathbf{u}_h^n, \nabla \eta\right)_f \Big\} &= 0, \quad (70)
\end{aligned}
$$

$$
\begin{aligned}
&\left(J^{n+\frac{1}{2}}\mathbf{v}_h^{n+1},\xi\right)_f+\beta\left(\mathbf{v}_h^{n+1},\xi\right)_s-k_n\left(J^{n+1}p_h^{n+1}(\boldsymbol{F}^{n+1})^{-T},\operatorname{Grad}\xi\right)_s\\
&+\frac{k_n}{2}\Bigg\{\left(\frac{\partial\Psi}{\partial\boldsymbol{F}}(\operatorname{Grad}\mathbf{u}_h^{n+1}),\operatorname{Grad}\xi\right)_s+\mu\left(J^{n+1}\operatorname{Grad}\mathbf{v}_h^{n+1}(\boldsymbol{F}^{n+1})^{-1},\operatorname{Grad}\xi(\boldsymbol{F}^{n+1})^{-1}\right)_f\\
&\qquad+\left(J^{n+1}\operatorname{Grad}\mathbf{v}_h^{n+1}(\boldsymbol{F}^{n+1})^{-1}\mathbf{v}_h^{n+1},\xi\right)_f\Bigg\}\\
&\qquad-\frac{1}{2}\left(J^{n+1}\operatorname{Grad}\mathbf{v}_h^{n+1}(\boldsymbol{F}^{n+1})^{-1}(\mathbf{u}_h^{n+1}-\mathbf{u}_h^{n}),\xi\right)_f\\
&\qquad-\left(J^{n+\frac{1}{2}}\mathbf{v}_h^{n},\xi\right)_f-\beta\left(\mathbf{v}_h^{n},\xi\right)_s\\
&+\frac{k_n}{2}\Bigg\{\left(\frac{\partial\Psi}{\partial\boldsymbol{F}}(\operatorname{Grad}\mathbf{u}_h^{n}),\operatorname{Grad}\xi\right)_s+\mu\left(J^{n}\operatorname{Grad}\mathbf{v}_h^{n}(\boldsymbol{F}^{n})^{-1},\operatorname{Grad}\xi(\boldsymbol{F}^{n})^{-1}\right)_f\\
&+\left(J^{n}\operatorname{Grad}\mathbf{v}_h^{n}(\boldsymbol{F}^{n})^{-1}\mathbf{v}_h^{n},\xi\right)_f\Bigg\}+\frac{1}{2}\left(J^{n}\operatorname{Grad}\mathbf{v}_h^{n}(\boldsymbol{F}^{n})^{-1}(\mathbf{u}_h^{n+1}-\mathbf{u}_h^{n}),\xi\right)_f=0,
\end{aligned}
\tag{71}
$$

$$
\left(J^{n+1}-1,\gamma\right)_s+\left(J^{n+1}\operatorname{Grad}\mathbf{v}_h^{n+1}(\boldsymbol{F}^{n+1})^{-1},\gamma\right)_f=0. \tag{72}
$$

Using the basis of the spaces U_h, V_h, P_h as the test functions ζ, ξ, γ we obtain a nonlinear algebraic set of equations. In each time step we have to find $\mathbf{X} = (\mathbf{u}_h^{n+1}, \mathbf{v}_h^{n+1}, p_h^{n+1}) \in U_h \times V_h \times P_h$ such that

$$
\mathcal{F}(\mathbf{X}) = \mathbf{0}, \tag{73}
$$

where $\mathcal{F}$ represents the system (70–72).

3.5 Solution algorithm

The system (73) of nonlinear algebraic equations is solved using Newton method as the basic iteration. One step of the Newton iteration can be written as

$$
\mathbf{X}^{n+1} = \mathbf{X}^n - \left[\frac{\partial\mathcal{F}}{\partial\mathbf{X}}(\mathbf{X}^n)\right]^{-1}\mathcal{F}(\mathbf{X}^n) \tag{74}
$$

The convergence of this basic iteration can be characterized by the following statement.

Theorem 1 *Let $\mathbf{X}$ be a solution of $\mathbf{F}(\mathbf{X}) = 0$ and $\frac{\partial\mathbf{F}}{\partial\mathbf{X}}(\mathbf{X}^n)$ is invertible and locally Lipschitz continuous. Then, if $\mathbf{X}^0$ is sufficiently close to $\mathbf{X}$, the Newton algorithm has the following property*

$$
\|\mathbf{X}^{n+1} - \mathbf{X}\| \le c\|\mathbf{X}^n - \mathbf{X}\|^2. \tag{75}
$$

We can see that this gives us quadratic convergence provided that the initial guess is sufficiently close to the solution. To ensure the convergence globally some improvements of this basic iteration are used.

The dumped Newton method with line search improves the chance of convergence by adaptively changing the length of the correction vector. The solution update step in the Newton method (74) is replaced by

$$\mathbf{X}^{n+1} = \mathbf{X}^n + \omega\delta\mathbf{X}, \tag{76}$$

where the parameter ω is found such that certain error measure decreases. One of the possible choices for the quantity to decrease is

$$f(\omega) = \mathcal{F}(\mathbf{X}^n + \omega\delta\mathbf{X}) \cdot \delta\mathbf{X}. \tag{77}$$

Since we know

$$f(0) = \mathcal{F}(\mathbf{X}^n) \cdot \delta\mathbf{X}, \tag{78}$$

and

$$f'(0) = \left[\frac{\partial\mathcal{F}}{\partial\mathbf{X}}(\mathbf{X}^n)\right]\delta\mathbf{X} \cdot \delta\mathbf{X} = \mathcal{F}(\mathbf{X}^n) \cdot \delta\mathbf{X}, \tag{79}$$

and computing $f(\omega_0)$ for $\omega_0 = -1$ or ω_0 determined adaptively from previous iterations we can approximate $f(\omega)$ by a quadratic function

$$f(\omega) = \frac{f(\omega_0) - f(0)(\omega_0 + 1)}{\omega_0^2}\omega^2 + f(0)(\omega + 1). \tag{80}$$

Then setting

$$\tilde{\omega} = \frac{f(0)\omega_0^2}{f(\omega_0) - f(0)(\omega_0 + 1)}, \tag{81}$$

the new optimal step length $\omega \in [-1, 0]$ is

$$\omega = \begin{cases} -\dfrac{\tilde{\omega}}{2} & \text{if } \dfrac{f(0)}{f(\omega_0)} > 0, \\ -\dfrac{\tilde{\omega}}{2} - \sqrt{\dfrac{\tilde{\omega}^2}{4} - \tilde{\omega}} & \text{if } \dfrac{f(0)}{f(\omega_0)} \leq 0. \end{cases} \tag{82}$$

This line search can be repeated with ω_0 taken as the last ω until, for example, $f(\omega) \leq \frac{1}{2}f(0)$. By this we can enforce a monotonous convergence of the approximation $\mathbf{X}^n$.

An adaptive time-step selection was found to help in the nonlinear convergence. A heuristic algorithm was used to correct the time-step length according to the convergence of the nonlinear iterations in the previous time-step. If the convergence was close to quadratic, i.e. only up to three Newton steps were needed to obtain required precision, the time step could be slightly increased, otherwise the time-step length was reduced.

The structure of the Jacobian matrix $\frac{\partial\mathcal{F}}{\partial\mathbf{X}}$ is

$$\frac{\partial\mathcal{F}}{\partial\mathbf{X}}(\mathbf{X}) = \begin{pmatrix} A_{vv} & A_{vu} & B_v \\ A_{uv} & A_{uu} & B_u \\ B_v^T & B_u^T & 0 \end{pmatrix}, \tag{83}$$

1. Let $\mathbf{X}^n$ be some starting guess.

2. Set the residuum vector $\mathbf{R}^n = \mathcal{F}(\mathbf{X}^n)$ and the tangent matrix $\boldsymbol{A} = \frac{\partial \mathcal{F}}{\partial \mathbf{X}}(\mathbf{X}^n)$.

3. Solve for the correction $\delta\mathbf{X}$

$$\boldsymbol{A}\delta\mathbf{X} = \mathbf{R}^n.$$

4. Find optimal step length ω.

5. Update the solution $\mathbf{X}^{n+1} = \mathbf{X}^n - \omega\delta\mathbf{X}$.

Figure 4: One step of the Newton method with the line search.

and it can be computed by finite differences from the residual vector $\mathcal{F}(\mathbf{X})$

$$\left[\frac{\partial \mathcal{F}}{\partial \mathbf{X}}\right]_{ij}(\mathbf{X}^n) \approx \frac{[\mathcal{F}]_i(\mathbf{X}^n + \alpha_j \mathbf{e}_j) - [\mathcal{F}]_i(\mathbf{X}^n - \alpha_j \mathbf{e}_j)}{2\alpha_j}, \tag{84}$$

where $\mathbf{e}_j$ are the unit basis vectors in $\mathbb{R}^n$ and coefficients α_j are adaptively taken according to the change in the solution in the previous time step. Since we know the sparsity pattern of the Jacobian matrix in advance, it is given by the used finite element method, this computation can be done in an efficient way so that the linear solver remains the dominant part in terms of the cpu time.

The linear problems are solved by BiCGStab iterations with ILU preconditioner with allowed certain fill-in for the diagonal blocks. The algorithms used are described in Barrett et al. [1994] and the implementation was taken from Bramley and Wang [1997].

4 Mixture model formulation

In this section we formulate and propose a solution algorithm for a steady state, two-dimensional problem of stretched rectangular slab of solid-fluid mixture. Two or three dimensional problems for solid fluid mixtures in connection with hydrated biological tissue were recently presented in Spilker et al. [1988], Spilker and Suh [1990], Suh et al. [1991], Donzelli et al. [1992], Vermilyea and Spilker [1993], Almeida and Spilker [1998] for biphasic mixture to model behavior of articular cartilage under compression. In all these works the nonlinear inertial of the fluid is neglected.

4.1 Model formulation

Let $\mathbf{u}$ denotes the solid displacement, $\mathbf{v} = \mathbf{v}^f$ denotes the fluid velocity while $\mathbf{v}^s = \mathbf{0}$ due to the assumption of a steady state, ϕ is the fluid volume fraction and p is the Lagrange multiplier associated with the incompressibility constraint. The interaction between the elastic material and the perfusing fluid is realized by the drag force in the form

$$\alpha\phi(1-\phi)(\mathbf{v}^f - \mathbf{v}^s). \tag{85}$$

which in the case of steady solution reduces to $\alpha\phi(1-\phi)\mathbf{v}$.

Our task is to find $(\mathbf{u}, \mathbf{v}, \phi, p)$ such that

$$\phi(\nabla\mathbf{v})\mathbf{v} + \nabla p - \operatorname{div}\boldsymbol{\sigma}^s = 0 \tag{86}$$

$$(\nabla\mathbf{v})\mathbf{v} + \nabla(p+\Psi) - \operatorname{div}\boldsymbol{\sigma}^f + (1-\phi)\boldsymbol{\alpha}\mathbf{v} = 0 \tag{87}$$

$$(1-\phi)\det\boldsymbol{F} = \phi_0^s \tag{88}$$

$$\operatorname{div}(\phi\mathbf{v}) = 0 \tag{89}$$

holds in domain Ω, where ϕ_0^s is the volume fraction of the solid in the reference state and the Helmholtz potential Ψ is given by constitutive equation as a function of ϕ and $\boldsymbol{F}$. The Cauchy stress tensor $\boldsymbol{\sigma}^s$ is then given by

$$\boldsymbol{\sigma}^s = (\phi + \beta(1-\phi))\frac{\partial\Psi}{\partial\boldsymbol{F}}\boldsymbol{F}^T, \tag{90}$$

where $\beta = \frac{\varrho_t^s}{\varrho_t^f}$ is the true mass ratio. By $\boldsymbol{S}$ we will denote the Piola-Kirchoff stress tensor

$$\boldsymbol{S} = -p(\det\boldsymbol{F})\boldsymbol{F}^{-T} + (\phi + \beta(1-\phi))(\det\boldsymbol{F})\frac{\partial\Psi}{\partial\boldsymbol{F}}. \tag{91}$$

Let the boundary $\partial\Omega$ be divided into three disjoint parts $\partial\Omega = \bigcup_{i=1}^3 \Gamma_i$. Let $\mathbf{n}$ be the unit normal vector to the boundary $\partial\Omega$. Then if $\mathbf{t}$ is given traction on the boundary, $\mathbf{u}_B$ is given solid boundary displacement and $\mathbf{v}_B$ is given fluid velocity at the boundary the possible boundary conditions are

$$\frac{1}{3}\operatorname{tr}\boldsymbol{\sigma} = p_B, \quad \mathbf{u} = \mathbf{u}_B \quad \text{ on } \Gamma_1, \tag{92}$$

$$-p\mathbf{n} + \boldsymbol{\sigma}^s\mathbf{n} = \mathbf{t}, \quad \mathbf{v} = \mathbf{v}_B \quad \text{ on } \Gamma_2, \tag{93}$$

$$\mathbf{u} = \mathbf{u}_B, \quad \mathbf{v} = \mathbf{v}_B \quad \text{ on } \Gamma_3. \tag{94}$$

We avoid prescribing partial stresses on the boundary since it is not clear weather such values can be obtained by measurements or how it should be partitioned into the partial stresses. Instead, we focus on the prescription of the fluid velocity at the boundary. There are other possible boundary conditions, apart of prescribing the fluid velocity. We may prescribe

$$\phi\mathbf{v} = \mathbf{f}_B, \tag{95}$$

or the total fluid flux through certain part of the boundary

$$\int_\Gamma \phi\mathbf{v}\cdot\mathbf{n}da = f_B, \tag{96}$$

which would be convenient as an outflow boundary condition. On the other hand the implementation of these conditions in the solution process is more complicated.

4.2 Weak formulation

In order to apply the finite element method we formulate our problem in a weak sense. Let us define spaces U, V, M and P as follows

$$U = \{\mathbf{u} \in [W^{1,2}(\Omega^s)]^2, \mathbf{u} = \mathbf{0} \text{ on } \Gamma_1 \cup \Gamma_3\} \tag{97}$$

$$V = \{\mathbf{v} \in [W^{1,2}(\Omega^s)]^2, \mathbf{v} = 0 \text{ on } \Gamma_2 \cup \Gamma_3\} \tag{98}$$

$$M = \{\phi \in W^{1,2}(\Omega^s)\} \tag{99}$$

$$P = \{p \in L^2(\Omega^s)\} \tag{100}$$

Multiplying equations (86)–(89) by a test functions $(\zeta, \xi, \eta, \gamma)$, integrating over the domain Ω and transforming the integration to the reference domain Ω^s yields

$$\int_{\Omega^s} \phi \nabla \mathbf{v} \operatorname{cof} \boldsymbol{F}^T \mathbf{v} \cdot \zeta dX - \int_{\Omega^s} p \operatorname{cof} \boldsymbol{F} \cdot \nabla \zeta dX + \int_{\Omega^s} \boldsymbol{S}^E \cdot \nabla \zeta dX - \int_{\Gamma_2} \mathbf{t} \operatorname{cof} \boldsymbol{F} \mathbf{N} \cdot \zeta dA = 0, \tag{101}$$

$$\begin{aligned} \int_{\Omega^s} \nabla \mathbf{v} \operatorname{cof} \boldsymbol{F} \mathbf{v} \cdot \xi dX - \int_{\Omega^s} (p + \Psi) \operatorname{cof} \boldsymbol{F} \cdot \nabla \xi dX + \int_{\Omega^s} (1 - \phi) \boldsymbol{\alpha} \mathbf{v} \cdot \xi \det \boldsymbol{F} dX \\ + \int_{\Gamma_1} (p_B - \frac{1}{3} \operatorname{tr} \boldsymbol{\sigma} + \Psi) \operatorname{cof} \boldsymbol{F} \mathbf{N} \cdot \xi dA = 0, \end{aligned} \tag{102}$$

$$\int_{\Omega^s} ((1 - \phi) \det \boldsymbol{F} - \phi_0^s)\, \eta dX = 0, \tag{103}$$

$$\int_{\Omega^s} \nabla(\phi \mathbf{v}) \cdot \operatorname{cof} \boldsymbol{F} \gamma dX = 0, \tag{104}$$

where $\operatorname{cof} \boldsymbol{F} = \det \boldsymbol{F} \boldsymbol{F}^{-T}$ and the inner product for two tensors is defined as $\boldsymbol{F} \cdot \boldsymbol{G} = \operatorname{tr}(\boldsymbol{F}^T \boldsymbol{G})$. Then our task is to find $(\mathbf{u}, \mathbf{v}, \phi, p)$ such that $(\mathbf{u} - \mathbf{u}_B, \mathbf{v} - \mathbf{v}_B, \phi, p) \in U \times V \times M \times P$ and equations (101)–(104) are satisfied for all $(\zeta, \xi, \eta, \gamma) \in U \times V \times M \times P$.

4.3 Discretization

We apply the same discretization and solution technique as in the previous section. The reference domain Ω^s is approximated by a domain Ω_h with piecewise linear boundary. The interior is divided by regular quadrilateral mesh into convex quadrilateral elements. The set of all quadrilaterals in Ω_h is denoted by $\mathcal{T}_h$ and $\tilde{T} = (-1, 1)^2$ is the reference quadrilateral. For each element $T \in \mathcal{T}_h$ there is a bilinear one to one mapping on to the reference element $\tilde{T}$. The spaces

U, V, M resp. P are approximated by the following finite element spaces

$$U_h = \{\mathbf{u}_h \in [C(\Omega_h)]^2, \mathbf{u}_h/T \in [Q_2(T)]^2 \quad \forall T \in \mathcal{T}_h, \mathbf{u}_h = \mathbf{0} \text{ on } \Gamma_1 \cup \Gamma_3\}, \tag{105}$$

$$V_h = \{\mathbf{v}_h \in [C(\Omega_h)]^2, \mathbf{v}_h/T \in [Q_2(T)]^2 \quad \forall T \in \mathcal{T}_h, \mathbf{v}_h = 0 \text{ on } \Gamma_1 \cup \Gamma_3\}, \tag{106}$$

$$M_h = \{\phi_h \in C(\Omega_h), \phi_h/T \in Q_1(T) \quad \forall T \in \mathcal{T}_h, 0 \leq \phi_h \leq 1\}, \tag{107}$$

$$P_h = \{p_h \in C(\Omega_h), p_h/T \in Q_1(T) \quad \forall T \in \mathcal{T}_h\}. \tag{108}$$

The resulting discrete problem is obtained by taking usual nodal basis of the space $U_h \times V_h \times M_h \times P_h$ and using the elements of this basis as test functions $(\zeta, \xi, \eta, \gamma)$ in (101–104). This set of non-linear algebraic equations can be written as

$$\mathcal{F}(\mathbf{X}) = \mathbf{0}, \tag{109}$$

where $\mathbf{X} = (\mathbf{u}_h, \mathbf{v}_h, \phi_h, p_h)$ is the vector of unknown components.

The Jacobian matrix $\left[\frac{\partial \mathcal{F}}{\partial \mathbf{X}}(\mathbf{X})\right]$ has following structure

$$\left[\frac{\partial \mathcal{F}}{\partial \mathbf{X}}(\mathbf{X})\right] = \begin{pmatrix} \boldsymbol{A}_{u,u} & \boldsymbol{A}_{u,v} & \boldsymbol{B}_{u,\phi} & \boldsymbol{C} \\ \boldsymbol{A}_{v,u} & \boldsymbol{A}_{v,v} & \boldsymbol{B}_{v,\phi} & \boldsymbol{C} \\ (1-\phi)\boldsymbol{C}^T & \mathbf{0} & \boldsymbol{B}_{\phi,\phi} & \mathbf{0} \\ \boldsymbol{A}_{p,u} & \phi\boldsymbol{C}^T & \boldsymbol{B}_{p,\phi} & \mathbf{0} \end{pmatrix} \tag{110}$$

This matrix has typical structure of constraint system with zero diagonal block.

4.4 Solution algorithm

The system (109) of nonlinear algebraic equations is again solved using the same approach like in the previous section. Additionally, since we seek the steady solution in this case, the continuation method is employed in order to have the starting approximation in the Newton iteration in the range of convergence. In the continuation method the problem $\mathbf{F}(\mathbf{X}) = 0$ is replaced by

$$\mathbf{G}(\mathbf{X}, \lambda) = 0 \tag{111}$$

where λ is a parameter such that for $\mathbf{G}(\mathbf{X}, 0) = 0$ we know the solution, while for $\lambda = 1$ the original problem is recovered

$$\mathbf{G}(\mathbf{X}, 1) \equiv \mathbf{F}(\mathbf{X}). \tag{112}$$

For example making the boundary conditions to depend on the parameter λ in such a way that for $\lambda = 0$ we have the undeformed, stress free state, and for $\lambda = 1$ we have the original boundary conditions.

In the process of the continuation method, we follow the solution curve given by the initial value problem

$$\frac{d}{ds}\mathbf{G}(\mathbf{X}(s), \lambda(s)) = 0, \tag{113}$$

$$(\mathbf{X}(0), \lambda(0)) = (\mathbf{X}_0, 0), \tag{114}$$

1. Let $\mathbf{X}^n$ be given starting approximation and λ^n the value of the continuation parameter.

2. Predictor step. Solve for $(\dot{\mathbf{X}^n}, \dot{\lambda^n})$

$$\left[\frac{\partial \mathbf{G}}{\partial \mathbf{X}}(\mathbf{X}^n, \lambda^n)\right] \dot{\mathbf{X}^n} + \left[\frac{\partial \mathbf{G}}{\partial \lambda}(\mathbf{X}^n, \lambda^n)\right] \dot{\lambda^n} = 0, \tag{115}$$

$$\|(\dot{\mathbf{X}^n}, \dot{\lambda^n})\| = 1. \tag{116}$$

3. Update the solution $(\mathbf{X}^{n+\frac{1}{2}}, \lambda^{n+1}) = (\mathbf{X}^n, \lambda^n) + \omega(\dot{\mathbf{X}^n}, \dot{\lambda^n})$.

4. Correction step. Solve for $\mathbf{X}^{n+1}$ by Newton iteration with $\mathbf{X}^{n+\frac{1}{2}}$ as starting guess

$$\mathbf{G}(\mathbf{X}^{n+1}, \lambda^{n+1}) = 0. \tag{117}$$

Figure 5: One step of Euler-Newton algorithm.

until the point $\lambda(s) = 1$. The basic method used to solve this problem is the Euler-Newton iteration, outlined in figure 5, where the explicit Euler method is applied to (113) as predictor and then the solution is corrected by the Newton method. This step is repeated until $\lambda^n = 1$. The parameter ω in the update step can be fixed or can be chosen adaptively, for example depending on the number of Newton iterations in the correction step needed to correct the solution.

The Jacobian matrix is computed again via finite differences. To invert the matrices in the most inner loops, BiCGStab or GMRES methods are used with preconditioning. See Barrett et al. [1994], Bramley and Wang [1997] for further details on these methods. The incomplete LU decomposition is used for preconditioning with suitable ordering of the unknowns and with fill-in allowed for certain pattern in the zero diagonal block of the jacobian matrix.

5 Applications

In this section we present a few example application to demonstrate the presented methods. As a motivation we consider the numerical simulation of the cardiovascular hemodynamics which has become a useful tool for deeper understanding of the onset of diseases of the human circulatory system, as for example blood cell and intima damages in stenosis, aneurysm rupture, evaluation of the new surgery techniques of heart, arteries and veins.

In order to test the proposed numerical method a simplified two-dimensional examples which include some of the important characteristics of the biomechanical applications are computed. The first example is a flow in an ellipsoidal cavity and the second is a flow through a channel with elastic walls. In both cases the

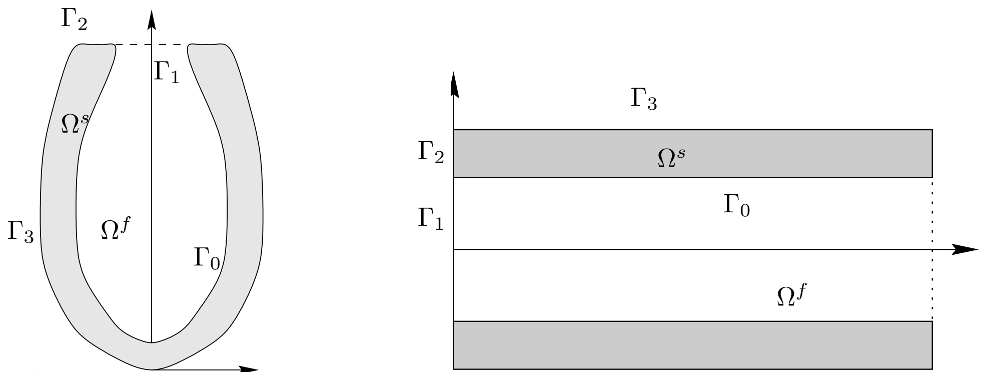

Figure 6: Schematic view of the ventricle and elastic tube geometries.

flow is driven by changing fluid pressure at the inflow part of the boundary while the elastic part of the boundary is either fixed or stress free.

The constitutive relations used for the materials are the incompressible Newtonian model (52) for the fluid and the hyper-elastic neo-Hookean material (58) with $c_2 = 0$ for the solid. This choice includes all the main dificulties the numerical method has to deal with, namely the incompressibility and large deformations.

5.1 Flow in an ellipsoidal cavity

The motivation for our first test is the left heart ventricle which is approximately ellipsoidal void surrounded by the heart muscle. In our two-dimensional computations we use an ellipsoidal cavity, see figure 6, with prescribed time-dependent natural boundary condition at the fluid boundary part Γ^1.

$$p(t) = \sin t \quad \text{on } \Gamma^1 \tag{118}$$

The material of the solid wall is modeled by the simple neo-Hookean constitutive relation (58) with $c_2 = 0$.

The figures 7 and 8 show the computational grid for the maximal and minimal volume configuration of the cavity and the velocity field of the fluid for the same configurations. One of the important characteristics is the shear stress exerted by the fluid flow on the wall material. This figure 8 shows the distribution of the shear stress in the domain for three different times. In figures 9 and 10 the volume change of the cavity as a function of the time and the average pressure inside the cavity versus the volume of the cavity is shown together with the trajectory and velocity of a material point on the solid fluid interface. We can see that after the initial cycle which was started from the undeformed configuration the system comes to a time periodic solution.

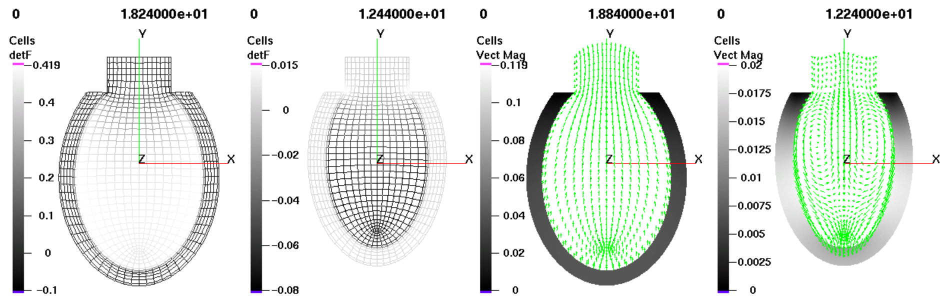

Figure 7: Maximum and minimum volume configuration with the fluid flow

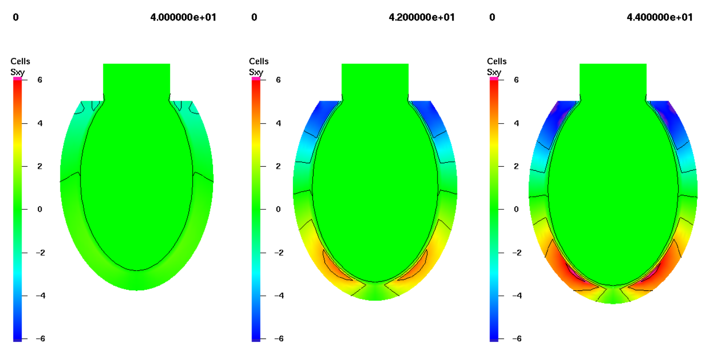

Figure 8: Shear stress distribution in the wall during the period.

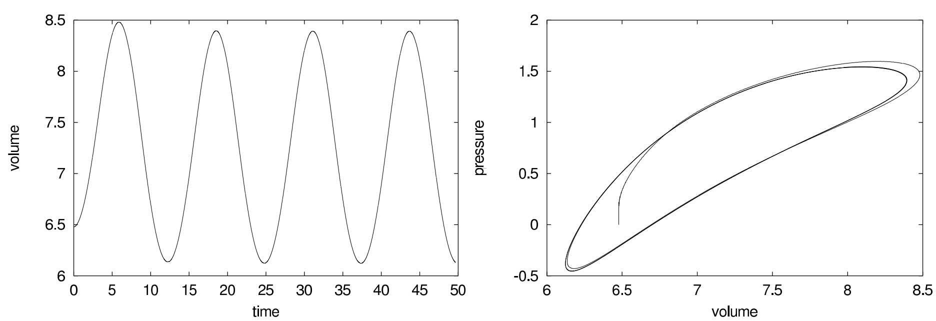

Figure 9: Volume of the fluid inside and the pressure-volume diagram for the ellipsoidal cavity test.

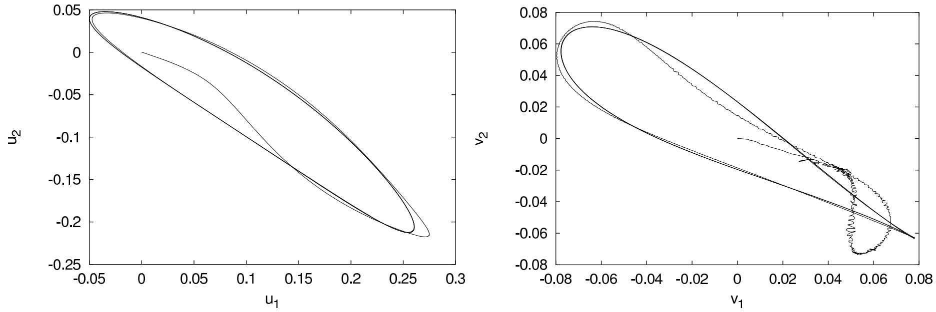

Figure 10: The displacement trajectory and velocity of a point at the fluid solid interface (inner side of the wall) for the ellipsoidal cavity test

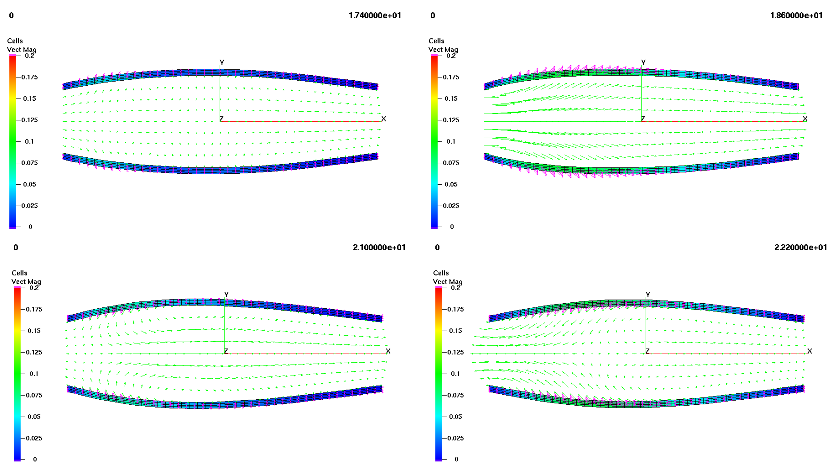

Figure 11: Velocity field during one pulse in channel without an obstacle

5.2 Flow in an elastic channel

The second application is the simulation of a flow in an elastic tube or in our 2 dimensional case a flow between elastic plates. The flow is driven by a time-dependent pressure difference between the ends of the channel of the form (118). Such flow is also interesting to investigate in the presence of some constriction as a stenosis, which is shown in figures 14.

For the flow in the channel without any constriction the time dependence of the fluid volume inside the channel is shown together with the pressure volume diagram in the figure and the trajectory and velocity of a material point on the solid fluid interface in the figures 12 and 13. The velocity field is shown in figure 11 at different stages of the pulse.

Finally in figure 14 the velocity field in the fluid and the pressure distribution throughout the wall is shown for the computation of the flow in a channel with

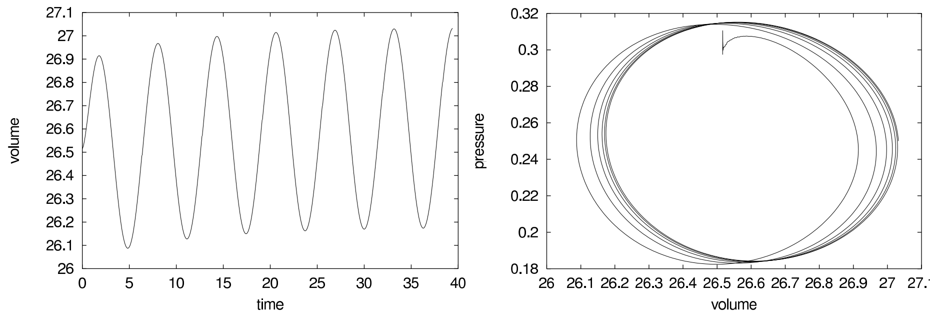

Figure 12: Volume of the fluid in the channel and the pressure-volume diagram.

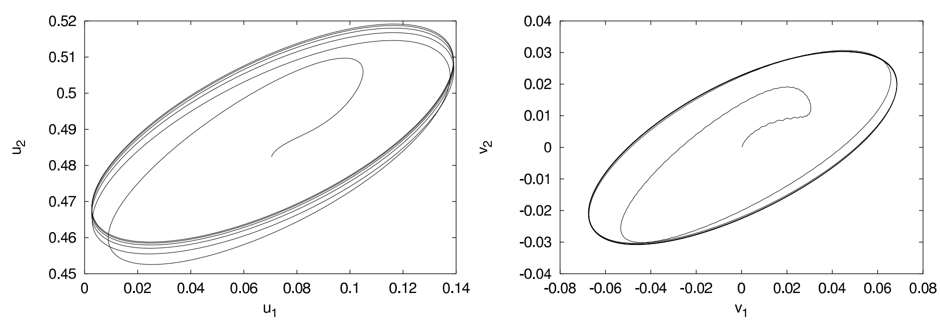

Figure 13: Displacement trajectory and velocity of a point at the fluid solid interface (inner side of the wall).

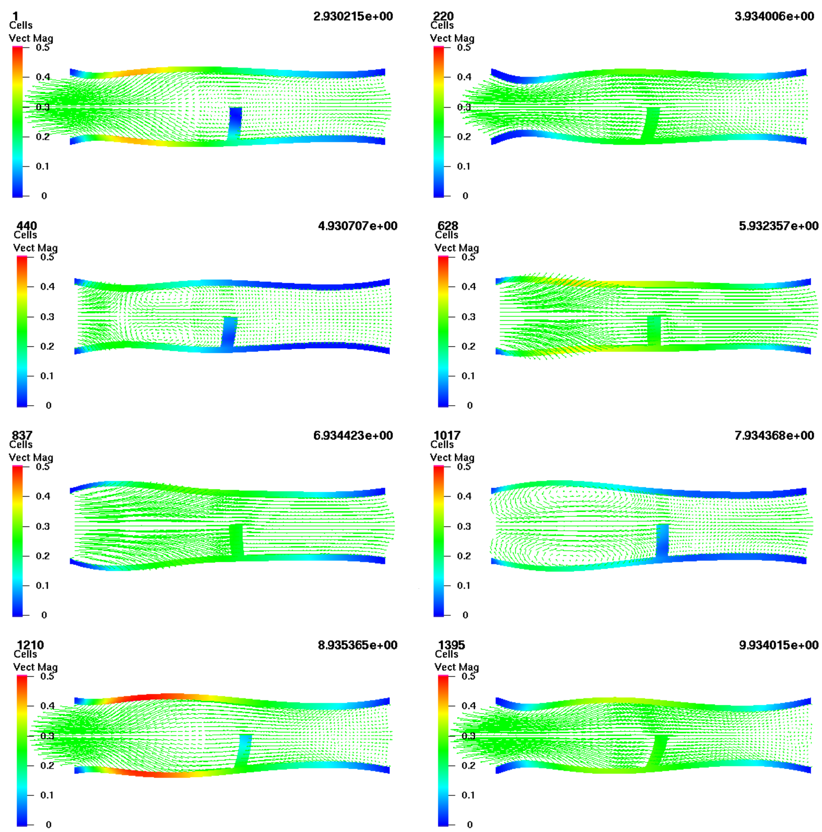

Figure 14: Fluid flow and pressure distribution in the wall during one pulse for the example flow in a channel with constriction

elastic obstruction. In this example the elastic obstruction is modeled by the same material as the walls of the channel and is fixed to the elastic walls. Both ends of the walls are fixed at the inflow and outflow and the flow is again driven by a periodic change of the pressure at the left end.

5.3 Illustrative example of perfusion

We take two dimensional crossection of the slab along the direction of the perfusion. Let $\Omega^s = [-L, L] \times [-H, H] \times [-L, L]$ be the reference domain occupied by the solid. The deformed domain, shown in figure 15, is

$$\Omega = \{x = X + \mathbf{u}(X), \forall X \in \Omega^s\}. \tag{119}$$

The deformation is assumed to be of a form

$$x_1 = X_1 + u_1(X_1, X_2), \qquad x_2 = X_2 + u_2(X_1, X_2), \qquad x_3 = \lambda_3 X_3, \tag{120}$$

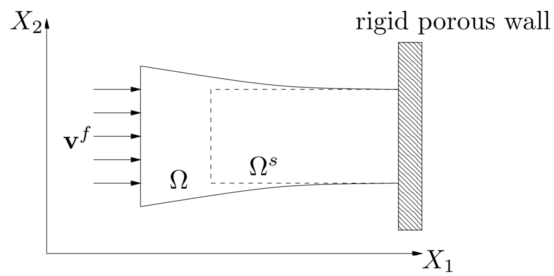

Figure 15: Undeformed and deformed configuration in two dimensional problem.

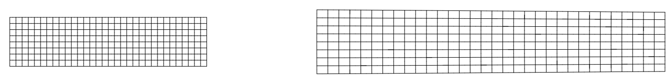

Figure 16: Finite element grid on the reference and the deformed configuration of the solid.

where λ_3 is prescribed positive constant. The fluid velocity is assumed to be

$$\mathbf{v}(x_1) = (v_1(x_1, x_2), v_2(x_1, x_2), 0). \tag{121}$$

The constitutive relation for the Helmholtz potential is used in the form

$$\Psi = c_1(I_C - 3) + c_2 \ln(\phi). \tag{122}$$

The boundary conditions applied are $\boldsymbol{\sigma}\mathbf{n} = \mathbf{t}$, $\phi\mathbf{v} = \mathbf{v}_B$ at the left end of the speciment, $u_1 = 0$, $\sigma_{12} = 0$, $\frac{1}{3}\operatorname{tr}\boldsymbol{\sigma} = p_B$ at the right end and $\boldsymbol{\sigma}\mathbf{n} = \mathbf{0}$, $\phi\mathbf{v} = \mathbf{v}_B$ the top and bottom boundaries.

In figure 16 is shown the finite element grid on the reference configuration of the solid. The initial solution is taken to be zero displacement and velocity, given constant volume fraction and Lagrange multiplier p such that the solution is stress free. The the solution for required values of the boundary conditions is computed by continuation. In figure 16 the finite element grid on the deformed configuration of the solid is shown. We can see that the slab becomes thicker in the X_2 direction at the left end, and thinner at the fluid outflow end. This variation in the thickness is caused by the gradual decrease in the pressure along the fluid flow. Figure 17 shows the velocity field of the perfusion and and the fluid volume fraction throughout the slab. The fluid velocity increases toward the end of the slab while the volume fraction decreases. In figure 18 the pressure field is shown together with the stress tensor components. We can notice the presence of stress concentration around the corners of the slab where the type of the boundary condition changes.

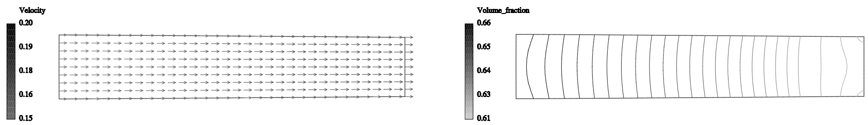

Figure 17: Fluid velocity and the fluid volume fraction.

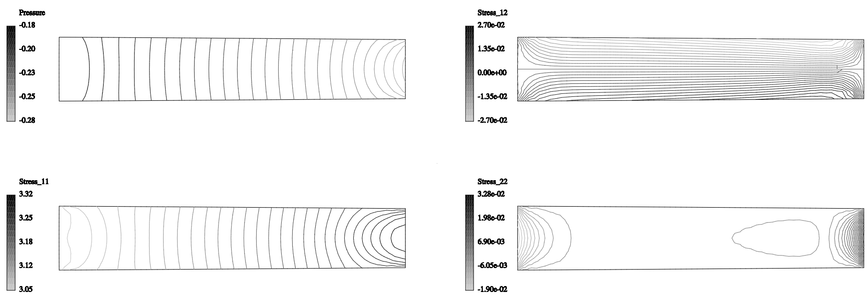

Figure 18: Isolines of the pressure field and the stress components σ_{12}, σ_{11} and σ_{22}.

6 Summary and future development

In this paper we present a general formulation of dynamic fluid-structure interaction problem suitable for applications with finite deformations and laminar flows. While the presented example calculations are simplified to allow initial testing of the numerical methods the formulation is general to allow immediate extension to more realistic material models. For example in the case of material anisotropy one can consider

$$\tilde{\Psi} = c_1(I_C - 3) + c_2(II_C - 3) + c_3(|\boldsymbol{F}\mathbf{a}| - 1)^2,$$

with $\mathbf{a}$ being the preferred material direction. The term $|\boldsymbol{F}\mathbf{a}|$ represents the extension in the direction $\mathbf{a}$. In Humphrey et al. [1990a,b] a similar material relation of the form

$$\tilde{\Psi} = c_1 \left(\exp\left(b_1(I_C - 3)\right) - 1\right) + c_2 \left(\exp\left(b_2(|\boldsymbol{F}\mathbf{a}| - 1)\right) - 1\right)$$

has been proposed to describe a passive behavior of the muscle tissue. Adding to any form of Ψ a term like $f(t, \mathbf{x})(|\boldsymbol{F}\mathbf{a}| - 1)$ one can model the active behavior of a material and then the system can be coupled with additional models of chemical and electric activation of the active response of the tissue, see Maurel et al. [1998]. In the same manner the constitutive relation for the fluid can be directly extended to the power law models used to describe the shear thinning property of the blood. Further extension to viscoelastic models and coupling with the mixture based model for soft tissues together with models for chemical and electric processes involved in biomechanical problems would allow to perform realistic simulation for real applications.

To obtain the solution approximation the discrete systems resulting from the finite element discretization of the governing equations need to be solved which requires sophisticated solvers of nonlinear systems and fast solvers for very large linear systems. The computational complexity increases tremendously for full 3D problems and with more complicated models like visco-elastic materials for the fluid or solid components. The main advantage of the presented numerical method is its accuracy and robustness with respect to the constitutive models. The possible directions of improving the efficiency of the solvers include development of fast linear solver based on multigrid ideas, spatial and temporal adaptivity and effective use parallel computations.

References

E. S. Almeida and R. L. Spilker. Finite element formulations for hyperelastic transversely isotropic biphasic soft tissues. *Comp. Meth. Appl. Mech. Engng.*, 151:513–538, 1998.

R. Barrett, M. Berry, T. F. Chan, J. Demmel, J. Donato, J. Dongarra, V. Eijkhout, R. Pozo, C. Romine, and H. Van der Vorst. *Templates for the solution of linear systems: Building blocks for iterative methods*. SIAM, Philadelphia, PA, second edition, 1994.

R. Bramley and X. Wang. *SPLIB: A library of iterative methods for sparse linear systems*. Department of Computer Science, Indiana University, Bloomington, IN, 1997. `http://www.cs.indiana.edu/ftp/bramley/splib.tar.gz`.

K. D. Costa, P. J. Hunter, R. J. M., J. M. Guccione, L. K. Waldman, and A. D. McCulloch. A three-dimensional finite element method for large elastic deformations of ventricular myocardium: I – Cylindrical and spherical polar coordinates. *Trans. ASME J. Biomech. Eng.*, 118(4):452–463, 1996a.

K. D. Costa, P. J. Hunter, J. S. Wayne, L. K. Waldman, J. M. Guccione, and A. D. McCulloch. A three-dimensional finite element method for large elastic deformations of ventricular myocardium: II – Prolate spheroidal coordinates. *Trans. ASME J. Biomech. Eng.*, 118(4):464–472, 1996b.

F. Dai and K. R. Rajagopal. Diffusion of fluids through transversely isotropic solids. *Acta Mechanica*, 82:61–98, 1990.

P. S. Donzelli, R. L. Spilker, P. L. Baehmann, Q. Niu, and M. S. Shephard. Automated adaptive analysis of the biphasic equations for soft tissue mechanics using a posteriori error indicators. *Int. J. Numer. Meth. Engng.*, 34 (3):1015–1033, 1992.

C. Farhat, M. Lesoinne, and N. Maman. Mixed explicit/implicit time integration of coupled aeroelastic problems: three-field formulation, geometric conservation and distributed solution. *Int. J. Numer. Methods Fluids*, 21(10): 807–835, 1995. Finite element methods in large-scale computational fluid dynamics (Tokyo, 1994).

Y. C. Fung. *Biomechanics: Mechanical properties of living tissues.* Springer-Verlag, New York, NY, 2nd edition, 1993.

M. E. Gurtin. *Topics in Finite Elasticity.* SIAM, Philadelphia, PA, 1981.

P. Haupt. *Continuum Mechanics and Theory of Materials.* Springer, Berlin, 2000.

M. Heil. Stokes flow in collapsible tubes: Computation and experiment. *J. Fluid Mech.*, 353:285–312, 1997.

M. Heil. Stokes flow in an elastic tube - a large-displacement fluid-structure interaction problem. *Int. J. Num. Meth. Fluids*, 28(2):243–265, 1998.

J. D. Humphrey, R. K. Strumpf, and F. C. P. Yin. Determination of a constitutive relation for passive myocardium: I. A new functional form. *J. Biomech. Engng.*, 112(3):333–339, 1990a.

J. D. Humphrey, R. K. Strumpf, and F. C. P. Yin. Determination of a constitutive relation for passive myocardium: II. Parameter estimation. *J. of Biomech. Engng.*, 112(3):340–346, 1990b.

B. Koobus and C. Farhat. Second-order time-accurate and geometrically conservative implicit schemes for flow computations on unstructured dynamic meshes. *Comput. Methods Appl. Mech. Engrg.*, 170(1-2):103–129, 1999.

M. K. Kwan, M. W. Lai, and V. C. Mow. A finite deformation theory for cartilage and other soft hydrated connective tissues - I. Equilibrium results. *J. Biomech.*, 23(2):145–155, 1990.

P. Le Tallec and S. Mani. Numerical analysis of a linearised fluid-structure interaction problem. *Num. Math.*, 87(2):317–354, 2000.

M. E. Levenston, E. H. Frank, and A. J. Grodzinsky. Variationally derived 3-field finite element formulations for quasistatic poroelastic analysis of hydrated biological tissues. *Comp. Meth. Appl. Mech. Engng.*, 156:231–246, 1998.

F. Maršík. *Termodynamika kontinua.* Academia, Praha, 1. edition, 1999.

F. Maršík and I. Dvořák. *Biothermodynamika.* Academia, Praha, 2. edition, 1998.

W. Maurel, Y. Wu, N. Magnenat Thalmann, and D. Thalmann. *Biomechanical models for soft tissue simulation.* ESPRIT basic research series. Springer-Verlag, Berlin, 1998.

M. I. Miga, K. D. Paulsen, F. E. Kennedy, P. J. Hoopes, and D. W. Hartov, A. Roberts. Modeling surgical loads to account for subsurface tissue deformation during stereotactic neurosurgery. In *IEEE SPIE Proceedings of Laser-Tissue Interaction IX, Part B: Soft-tissue Modeling*, volume 3254, pages 501–511, 1998.

C. W. J. Oomens and D. H. van Campen. A mixture approach to the mechanics of skin. *J. Biomech.*, 20(9):877–885, 1987.

K. D. Paulsen, M. I. Miga, F. E. Kennedy, P. J. Hoopes, A. Hartov, and D. W. Roberts. A computational model for tracking subsurface tissue deformation during stereotactic neurosurgery. *IEEE Transactions on Biomedical Engineering*, 46(2):213–225, 1999.

C. S. Peskin. Numerical analysis of blood flow in the heart. *J. Computational Phys.*, 25(3):220–252, 1977.

C. S. Peskin. The fluid dynamics of heart valves: experimental, theoretical, and computational methods. In *Annual review of fluid mechanics, Vol. 14*, pages 235–259. Annual Reviews, Palo Alto, Calif., 1982.

C. S. Peskin and D. M. McQueen. Modeling prosthetic heart valves for numerical analysis of blood flow in the heart. *J. Comput. Phys.*, 37(1):113–132, 1980.

C. S. Peskin and D. M. McQueen. A three-dimensional computational method for blood flow in the heart. I. Immersed elastic fibers in a viscous incompressible fluid. *J. Comput. Phys.*, 81(2):372–405, 1989.

A. Quarteroni. Modeling the cardiovascular system: a mathematical challenge. In B. Engquist and W. Schmid, editors, *Mathematics Unlimited - 2001 and Beyond*, pages 961–972. Springer-Verlag, 2001.

A. Quarteroni, M. Tuveri, and A. Veneziani. Computational vascular fluid dynamics: Problems, models and methods. *Computing and Visualization in Science*, 2(4):163–197, 2000.

K. R. Rajagopal and L. Tao. *Mechanics of mixtures*. World Scientific Publishing Co. Inc., River Edge, NJ, 1995.

R. A. Reynolds and J. D. Humphrey. Steady diffusion within a finitely extended mixture slab. *Math. Mech. Solids*, 3(2):127–147, 1998.

M. Rumpf. On equilibria in the interaction of fluids and elastic solids. In *Theory of the Navier-Stokes equations*, pages 136–158. World Sci. Publishing, River Edge, NJ, 1998.

P. A. Sackinger, P. R. Schunk, and R. R. Rao. A Newton-Raphson pseudo-solid domain mapping technique for free and moving boundary problems: a finite element implementation. *J. Comput. Phys.*, 125(1):83–103, 1996.

J. J. Shi. *Application of theory of a Newtonian fluid and an isotropic non-linear elastic solid to diffusion problems.* PhD thesis, University of Michigan, Ann Arbor, 1973.

R. L. Spilker and J. K. Suh. Formulation and evaluation of a finite element model for the biphasic model of hydrated soft tissues. *Comp. Struct., Front. Comp. Mech.*, 35(4):425–439, 1990.

R. L. Spilker, J. K. Suh, and V. C. Mow. Finite element formulation of the non-linear biphasic model for articular cartilage and hydrated soft tissues including strain-dependent permeability. *Comput. Meth. Bioeng.*, 9:81–92, 1988.

J. K. Suh, R. L. Spilker, and M. H. Holmes. Penalty finite element analysis for non-linear mechanics of biphasic hydrated soft tissue under large deformation. *Int. J. Numer. Meth. Engng.*, 32(7):1411–1439, 1991.

C. Truesdell. *A first course in rational continuum mechanics*, volume 1. Academic Press Inc., Boston, MA, second edition, 1991.

W. J. Vankan, J. M. Huyghe, J. D. Janssen, and A. Huson. Poroelasticity of saturated solids with an application to blood perfusion. *Int. J. Engng. Sci.*, 34(9):1019–1031, 1996.

W. J. Vankan, J. M. Huyghe, J. D. Janssen, and A. Huson. Finite element analysis of blood flow through biological tissue. *Int. J. Engng. Sci.*, 35(4): 375–385, 1997.

M. E. Vermilyea and R. L. Spilker. Hybrid and mixed-penalty finite elements for 3-d analysis of soft hydrated tissue. *Int. J. Numer. Meth. Engng.*, 36(24): 4223–4243, 1993.

C. Zoppou, S. I. Barry, and G. N. Mercer. Dynamics of human milk extraction: a comparitive study of breast-feeding and breast pumping. *Bull. Math. Biology*, 59(5):953–973, 1997.